

Timing and Spectroscopy of Accreting X-ray Pulsars: the State of Cyclotron Line Studies

W.A. Heindl*, R.E. Rothschild*, W. Coburn[†], R. Staubert**, J. Wilms **, I. Kreykenbohm^{‡**} and P. Kretschmar^{‡§}

*Center for Astrophysics and Space Sciences, University of California, San Diego

[†]Space Sciences Laboratory, University of California, Berkeley

**Institut für Astronomie und Astrophysik, Tübingen

[‡]INTEGRAL Science Data Center

[§]Max-Planck-Institut für Extraterrestrische Physik

Abstract. A great deal of emphasis on timing in the *RXTE* era has been on pushing toward higher and higher frequency phenomena, particularly kHz QPOs. However, the large areas of the *RXTE* pointed instruments provide another capability which is key for the understanding of accreting X-ray pulsars – the ability to accumulate high quality spectra in a limited observing time. For the accreting X-ray pulsars, with their relatively modest spin frequencies, this translates into an ability to study broad band spectra as a function of pulse phase. This is a critical tool, as pulsar spectra are strong functions of the geometry of the “accretion mound” and the observers’ viewing angle to the $\sim 10^{12}$ G magnetic field. In particular, the appearance of “cyclotron lines” is sensitively dependent on the viewing geometry, which must change with the rotation of the star. These spectral features, seen in only a handful of objects, are quite important, as they give us our only direct measure of neutron star magnetic fields. Furthermore, they carry a great deal of information as to the geometry and physical conditions in the accretion mound. In this paper, we review the status of cyclotron line studies with the *RXTE*. We present an overview of phase-averaged results and give examples of observations which illustrate the power of phase-resolved spectroscopy.

INTRODUCTION

In this work, we review the status of *RXTE* cyclotron line studies in the classical accreting X-ray pulsars and discuss the observational requirements needed to further our understanding in this area. We specifically do not consider the new class of *millisecond* accreting pulsars, as they are the subject of other papers in this proceedings.

Cyclotron lines, or more precisely “cyclotron resonance scattering features” (CRSFs) are formed at or near the neutron star magnetic polar cap where electron motions perpendicular to the field are quantized in Landau orbits. This gives rise to increased magnetic Compton scattering opacity at the (harmonically spaced) Landau energies resulting in absorption-line-like features in the emergent spectra. Owing to the $\sim 10^{12}$ G field strength, the Landau transitions have energies in the hard X-ray band: $E_{n,s} = (n + \frac{1}{2} + s)E_{\text{cyc}}$, where n is the principle quantum number, $s = \pm 1/2$ is the electron spin, and $E_{\text{cyc}} = \frac{\hbar e B}{m_e} = 11.6 \frac{B}{10^{12} \text{G}}$ keV. Thus, the cyclotron line energy gives a direct measure of the magnetic field in the scattering region. Of course, the observed line energy will be redshifted in the strong gravitational field of the neutron star such that $B_{12} = (1 + z) \frac{E_{\text{obs}}}{11.6 \text{keV}}$, where B_{12} is

the field strength in 10^{12} G and z is the redshift in the scattering region. In addition, when relativistic effects are considered [1] the line spacing is no longer expected to be harmonic: $E_{\text{cyc}} \propto [(1 + 2n \frac{B}{B_{\text{crit}}} \sin^2 \theta)^{1/2} - 1] / \sin^2 \theta$ where θ is viewing angle with respect to the magnetic field and $B_{\text{crit}} = m^2 c^3 / e \hbar = 4.4 \times 10^{13}$ G. For magnetic fields in the 10^{12} G range, these shifts are $\lesssim 10\%$.

These considerations lay down the basic theoretical principles for cyclotron line formation. However, the practical reality is that the situation is quite complex. Monte Carlo simulations by several authors (see e.g., [2, 3, 4]) show that when the physical geometry of the emitting region and the observing aspect are considered, complex line shapes, particularly for the fundamental, can be produced. Figure 1 is a schematic of the model geometry assumed by these Monte Carlo studies. The X-rays are produced in an “accretion mound”. This consists of an underlying continuum producing volume above which photons must propagate through a line forming region characterized by a magnetic field strength, electron temperature, and Thomson optical depth. In various models, the electron temperature, the geometry of the mound, the angle of the magnetic field with respect to the mound, and the injected continuum beam pattern can be var-

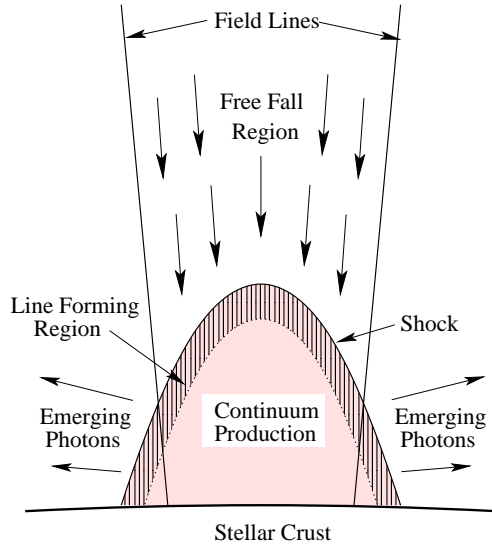


FIGURE 1. Schematic diagram of the “accretion mound” showing the line-forming region as a discrete layer covering the continuum production zone.

ied. Figure 2, (from [3]) compares predicted line shapes for various viewing angles for both slab and cylindrical mound geometries when continuum photons are injected isotropically and in a cone. In these models, the fundamental line only appears as a simple absorption feature in the case of a slab-shaped mound with isotropic injection viewed nearly perpendicular to the magnetic field axis. In some cases, the fundamental is flanked by apparent emission wings, and can even appear as an *emission* line. Furthermore, it is quite clear that the expected line shape is a strong function of viewing geometry. And, it is precisely this viewing angle which is changing as the neutron star rotates. Thus, it would be quite naive to expect to make a clean measurement of a cyclotron line without performing phase-resolved spectroscopy. Conversely, if the phase average spectrum does appear simple, then we can place limits on the variation of the viewing angle through the pulse.

RXTE PHASE-AVERAGE RESULTS

In this section, we give an overview of measurements of cyclotron lines using the *RXTE*. Table 1 lists all of the pulsars where cyclotron lines have been convincingly detected. The instrument which was used in the discovery of the line is given as well as whether the line has been detected with *RXTE*. A total of 14 pulsars have secure line detections, and all but two (V 0332+53 and A 0535+26: transients which have been inactive during the *RXTE* lifetime) have been measured. Furthermore,

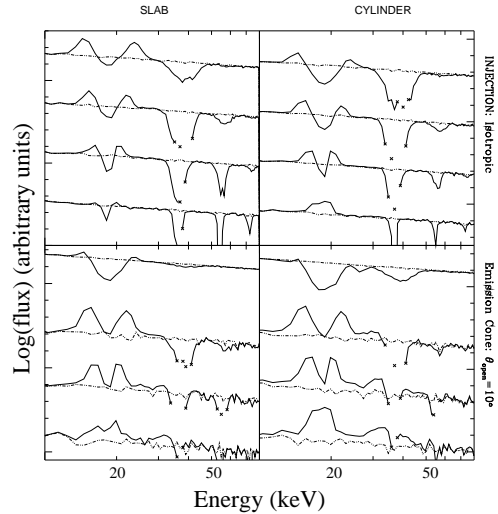


FIGURE 2. From [3]. Monte Carlo models of emergent photon spectra as a function of viewing angle, emission mound geometry, and continuum injection geometry. Each panel shows the injected (dashed line) and detected (solid line) spectra for four viewing angles ranging (top to bottom) from nearly parallel to nearly perpendicular to the magnetic field. The left panels are for a slab geometry accretion mound and the right panels are a cylindrical mound. Finally the top two panels are for isotropic continuum injection while the the bottom panels are for conical injection about the magnetic field direction.

five of the lines have been discovered with *RXTE* or with both *BeppoSAX* and *RXTE*.

MX 0656-072: A new line in an old transient

As an example of a cyclotron line seen in a phase averaged spectrum, we show the recent discovery of the line in MX 0656–07 (=XTE J0658–072). MX 0656–07 was discovered with SAS-3 in October 1975 [19] and was seen again with Ariel-V in March 1976 [20]. At the time, it was not recognized as a pulsar. The source became active again only in 2003 October [21], and an *RXTE* observation on 2003 October 19–20 revealed that it is a 160 s accreting pulsar [22]. Its optical counterpart is a Be star [23], making it one of the transient Be star/X-ray pulsar binaries. Analyzing the phase average spectrum from this observation, we discovered a cyclotron line at ~ 36 keV [15]. The spectrum is shown in Figure 3. We fit the continuum with a power law which breaks smoothly to a power law times an exponential cutoff at high energies (the “modified power law cutoff model”, MPL-CUT [24]). An iron line was also required. The cyclotron line is modeled by an absorption line with a Gaussian optical depth profile (see [24] for the exact functional

TABLE 1. List of pulsars with securely detected cyclotron lines. The discovery instrument is listed along with the discovery reference and whether the line has been observed with *RXTE*.

| Source | Energy (keV) | Discovery Instrument | <i>RXTE</i> ? |
|--------------------------|---------------|----------------------|---------------|
| 4U 0115+63 [†] | 12 [5] | <i>HEAO-1</i> | Y |
| 4U 1907+09 ^{†‡} | 18 [6] | <i>Ginga</i> | Y |
| 4U 1538–52 [‡] | 20 [7] | <i>Ginga</i> | Y |
| Vela X–1 ^{†‡} | 25 [8] | HEXE | Y |
| V 0332+53 | 27 [9] | <i>Ginga</i> | N |
| Cep X–4 | 28 [10] | <i>Ginga</i> | Y |
| Cen X–3 [‡] | 28.5 [11, 12] | <i>RXTE/BSAX</i> | Y |
| X Per | 29 [13] | <i>RXTE</i> | Y |
| XTE J1946+274 | 36 [14] | <i>RXTE/BSAX</i> | Y |
| MX0656–072 | 36 [15] | <i>RXTE</i> | Y |
| 4U 1626–67 | 37 [12, 16] | <i>RXTE/BSAX</i> | Y |
| GX 301–2 [‡] | 37 [6] | <i>Ginga</i> | Y |
| Her X–1 [‡] | 41 [17] | Balloon | Y |
| A 0535+26 | 50?, 110 [18] | HEXE | N |

[†] objects with > 1 harmonic observed

[‡] high inclination system

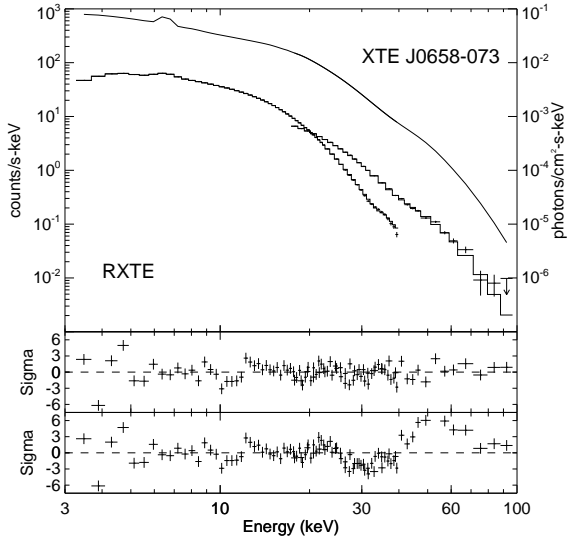


FIGURE 3. The phase average spectrum of MX 0656–072 observed with *RXTE*. The middle panel shows residuals for the full model including a cyclotron line, while the bottom panel is the best fit continuum with no cyclotron line. The line is apparent as the dip at ~ 30 keV and the underestimation of the continuum above 40 keV.

form). The best-fit line parameters are: $E_{\text{cyc}} = 36 \pm 1$ keV, $\sigma_{\text{cyc}} = 7.5 \pm 1.0$ keV, $\tau_{\text{cyc}} = 0.33 \pm 0.05$. σ_{cyc} and τ_{cyc} are the width and maximum of the optical depth profile.

Correlations of Spectral Parameters

Coburn [25] and Coburn *et al.* [24] examined the phase average spectra of all the pulsars observed with high statistics with *RXTE*. In the cases where no cyclotron line was found (12 objects), the authors placed upper limits on the width and optical depth of any line as a function of energy. In order to look for class-wide relationships among the 12 cyclotron line pulsars, they fit their spectra to the common spectral model (MPLCUT plus iron emission) including a cyclotron line as described above. They then searched for correlations between model parameters. Three significant correlations were noted: 1. between the cyclotron line energy and the continuum break energy, 2. between the width of the cyclotron line and its energy, and 3. between the fractional width of the cyclotron line and its depth. Figures 4–6 are plots of the fit parameters showing these three correlations. In these plots, the hashed regions indicate where *RXTE* is not sensitive to lines for typical source brightnesses and moderate observing times. The fact that the observed points do not fill the available phase space shows that the correlations are not selection effects. The first two of these correlations have been noted previously (1: [6], [26]; 2: [27], [28]), while the third is new. Importantly, this is the first time that these correlations have been demonstrated in a uniform analysis of data from a single set of instruments.

The correlation between cyclotron line energy and continuum break energy was originally noted by [6] and [26] who compared fit parameters from different missions. With the exception of A 0535+26 (plotted at

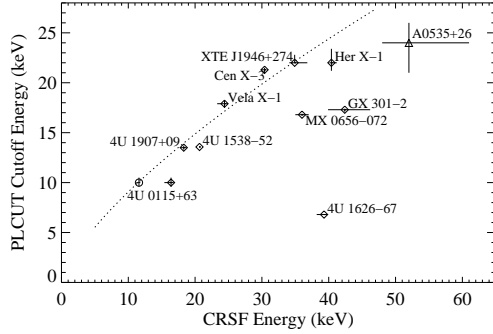


FIGURE 4. Continuum break energy plotted versus cyclotron line energy. After Figure 9 of [24]. Hashed regions indicate phase space where the *RXTE* is not sensitive to lines. Except for A 0535+26, all data points are from *RXTE*.

the lower of the two possible fundamental line energies [29]), all the data in Figure 4 come from *RXTE*. Below ~ 35 keV, the correlation appears clean. However, at higher line energies the case is not so clear. We discount 4U 1626-67, as its break energy is highly variable with pulse phase and so the phase average spectrum is a poor representation. However, this still leaves GX 301-2 and MX 0656-07 in poor agreement with the correlation. One possibility is that these sources are like Vela X-1. In Vela X-1, the strong observed line near 50 keV is in fact a harmonic, and phase resolved spectroscopy has confirmed (see below) that the fundamental is weak, lying near 25 keV. Moving the line energies down by a factor of two would bring GX 301-2 and MX 0656-07 in good agreement with the correlation. Another, perhaps more likely explanation is that, like 4U 1626-67, the phase average spectrum is misleading for these sources. Finally, of course, the correlation may simply break down at these energies. In any case, the correlation suggests that the continuum cutoff is a magnetic effect and that it is not the temperature of the accretion mound alone that determines the hardness of high energy spectrum.

To first order, a correlation between the line width and energy is expected. If the line width (Γ_{cyc}) is dominated by the temperature of the electrons (kT_e), then according to [30], $\Gamma_{cyc} \sim E_{cyc} \left(\frac{8 \ln(2) kT_e}{m_e c^2} \right)^{1/2} |\cos\theta|$. The fact that this correlation is observed, however, implies that there is neither a large variation in electron temperature nor in viewing angle, θ , from source to source. If there were, then the correlation should be destroyed. The stricture on $\cos\theta$ is quite interesting given the prevalence of high inclination systems among the cyclotron line pulsars (see Table 1). This suggests that the magnetic and spin axes in these systems tend to be nearly aligned, and that either they are born that way or that accretion tends to align them.

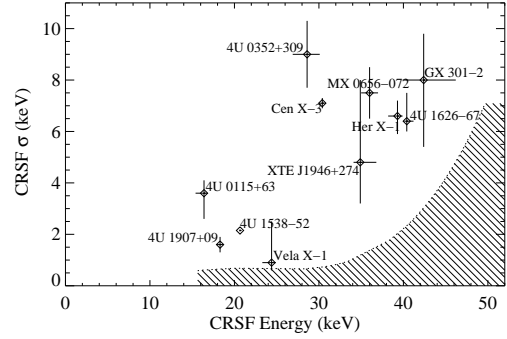


FIGURE 5. Cyclotron line width plotted versus cyclotron line energy. The width is the sigma of the Gaussian optical depth profile. After Figure 7 of [24]. Hashed regions indicate phase space where the *RXTE* is not sensitive to lines.

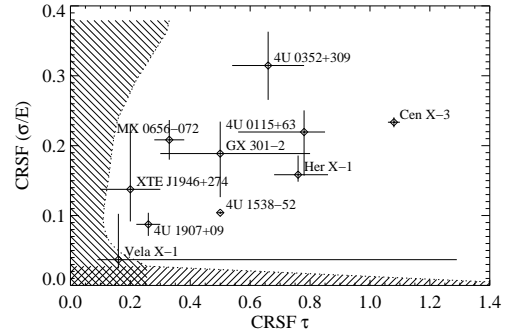


FIGURE 6. Fractional cyclotron line width plotted versus cyclotron line energy. The fractional width is the sigma of the Gaussian optical depth profile divided by the line energy. After Figure 8 of [24]. Hashed regions indicate phase space where the *RXTE* is not sensitive to lines.

The correlation between the fractional line width and energy is new and in fact quite surprising. This correlation says that broad lines tend to be deep and narrow lines tend to be shallow. However, both from simple considerations of the magnetic scattering cross sections at finite temperatures [2] and from Monte Carlo models (see Figure 2), it is the narrow lines that should be deep.

SELECTED *RXTE* PHASE-RESOLVED RESULTS

In this section, we discuss three pulsars where we have carried out pulse phase resolved spectroscopy. These observations show the power of the large collecting areas or the *RXTE* instruments to reveal detailed variations in the spectrum and hint at possibilities for a future mission that will perform such observations of much weaker pulsars.

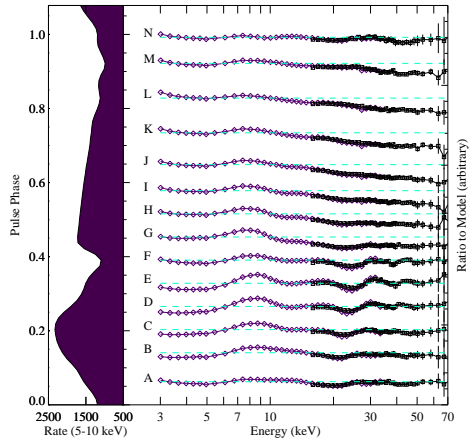


FIGURE 7. Normalized ratios of the *RXTE* data in 14 phase bins to a smooth continuum model. On the left, the corresponding pulse profile is plotted vertically. The dips in the ratios indicate the presence of multiple cyclotron line harmonics.

4U 0115+63

The Be/X-ray binary transient pulsar 4U 0115+63 was one of the earliest cyclotron line pulsars and was the first to show both a fundamental and a harmonic line [31]. It is still the pulsar with the lowest fundamental energy, making it the best candidate for multiple harmonics to be observed. In 1999 March-April, 4U 0115+63 underwent an outburst that was observed both with *RXTE* [32] and *BeppoSAX* [33]. The results from the two observatories are in good agreement. We present the *RXTE* results here. Figure 7 shows the spectrum as a function of pulse phase. At each of 14 phases corresponding to the pulse profile (plotted vertically), the PCA and HEXTE spectra are plotted, divided by a smooth continuum model and normalized to unit intensity. This reveals strong variability in the spectrum, both in overall hardness as well as in the presence of cyclotron lines. The wiggles (e.g., phase D) bely the presence of up to five cyclotron line harmonics. This is in fact the only source where more than two lines have been seen.

Detailed fitting of these spectra reveals that as many as five lines (the fundamental plus four harmonics) are detected. Figure 8 shows a fit to the phase D spectrum, with the required lines indicated. The fundamental has been fit with a complex shape, and its energy is hard to determine. As expected from theory, however, the rest of the lines follow a harmonic relationship with a spacing of half of the energy of the ~ 24 keV harmonic.

Finally, figure 9 shows the evolution of the first and second harmonic line energies with pulse phase. It is clear that we observe regions with a 20% range in mag-

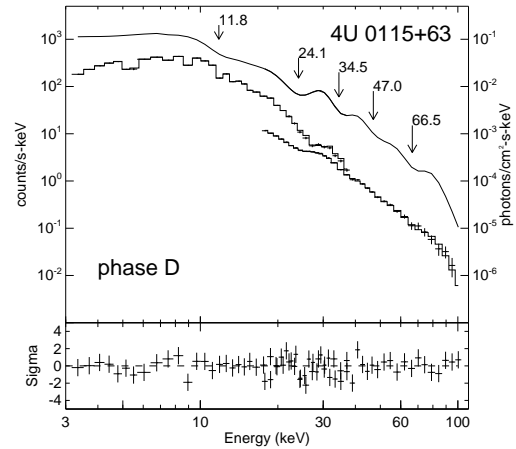


FIGURE 8.

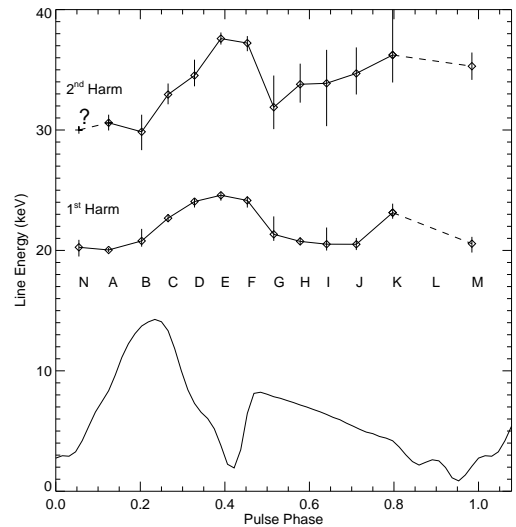


FIGURE 9. The energies of the 4U 0115+63 first and second harmonic lines as a function of pulse phase plotted above the arbitrarily normalized pulse profile. The harmonic relation of the line energies is maintained within statistics at all phases where the lines are detected.

netic field. This emphasizes the need for phase resolved spectroscopy as these variations are integrated in a phase average spectrum. Such variations could be due, for example, to quadrupole and higher field components or an offset of the dipole with respect to the center of the star.

Vela X-1

Vela X-1 is a 283 s pulsar in an 8.964 d orbit with a B0.5Ib supergiant. The radius of the orbit is only ~ 1.7 times the B star radius, and with this small separation, the neutron star accretes from the intense stellar wind.

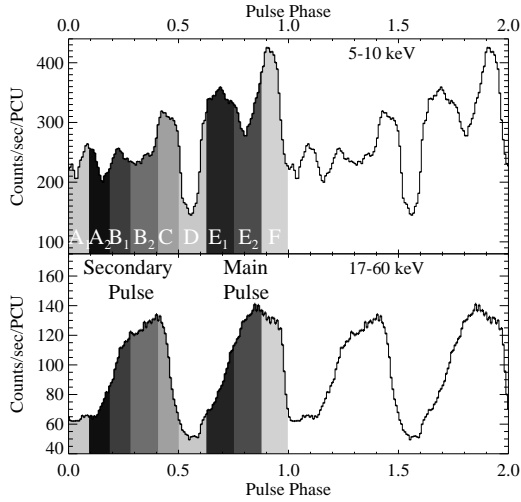


FIGURE 10. From [37]. The Vela X–1 pulse profile in two energy bands. The shaded regions indicate phase bins used for phase resolved spectroscopy (see figure 11).

Observations with HEXE on *Mir* [8], *Ginga* [34], *RXTE* [35], and *BeppoSAX* [36] all show evidence of a cyclotron line at ~ 50 keV. There have also been reports with *Ginga* [34] and HEXE [8] of a line near 24 keV. This line would be the fundamental, making the ~ 50 keV an harmonic. Observations with *BeppoSAX* have not confirmed this line. However, phase resolved observations with *RXTE* now find that there is a weak, phase variable line near 25 keV.

Figure 10 from [37] shows the Vela X–1 pulse profile in two energy bands from a 2000 January *RXTE* observation. The profile has two, simple main peaks at high energies that are subdivided into multiple peaks at low energies. The phase ranges for phase resolved spectroscopy are indicated. The evolution of cyclotron line parameters, for both the fundamental and the harmonic, is shown in figure 11. Note that, as indicated by the optical depth, the fundamental is not significantly detected over much of the secondary pulse. Indeed, this phase variability of the line is strong evidence that it is real and not an artifact of the spectral fitting. It is likely due to the combination of this pulse phase variability and the strongly time variable photoelectric absorption by the stellar wind (N_H can be well over 10^{23} cm^{-1}) that it has been difficult to confirm this line.

GX 301–2

The neutron star in GX 301–2 orbits the early type B-emission line star Wray 977. The 41.5 d orbit is eccentric ($e = 0.462$), and just prior to periastron passage the neutron star intercepts the gas stream from Wray 977

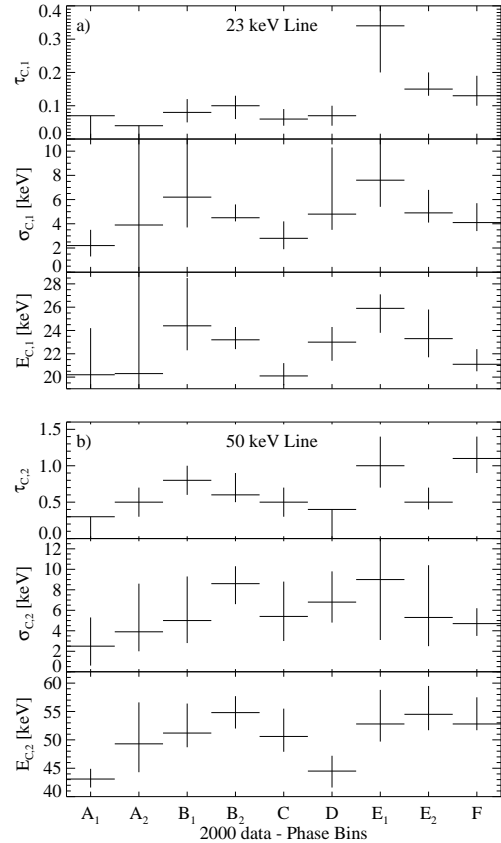


FIGURE 11. From [37]. Variations of the Vela X–1 fundamental and harmonic cyclotron line parameters with pulse phase for the phase bins defined in figure 10.

[38, 39], resulting in an extended X-ray flare. In 2000 October, Kreykenbohm et al. [40] made a long observation with *RXTE* spanning this pre-periastron flare. Figure 12 shows the resulting pulse profile along with the phase behavior of the cyclotron line parameters. Note the similarity of the pulse to Vela X–1. Both sources show a double-peaked profile with the two peaks having similar strength and shape. Again, the line energy is strongly variable, shifting by more than 20%.

Unlike Vela X–1, no cyclotron line is detected near the half energy of the strong deep line at ~ 35 keV. This leaves GX 301–2 a poor fit to the cutoff energy vs. cyclotron energy correlation (figure 4). However, the phase resolved points are a good fit to the other correlations. Figure 13 shows both the width–energy correlation and the relative width–depth correlation. The fact that these correlations are confirmed within a single object is good evidence that they are a physical result of the cyclotron line formation. Furthermore, if indeed the electron temperature is responsible for the line width, then we can infer that the range of viewing angles to the magnetic field is limited, varying only by roughly 12° as the star rotates

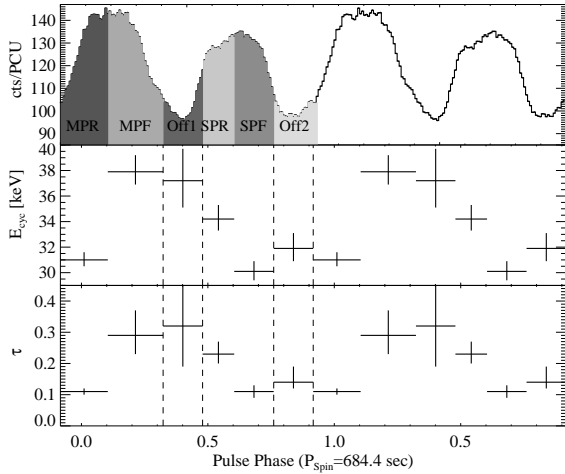


FIGURE 12. From [40]. The GX 301–2 pulse profile and phase resolved spectral fits of the cyclotron line energy and depth.

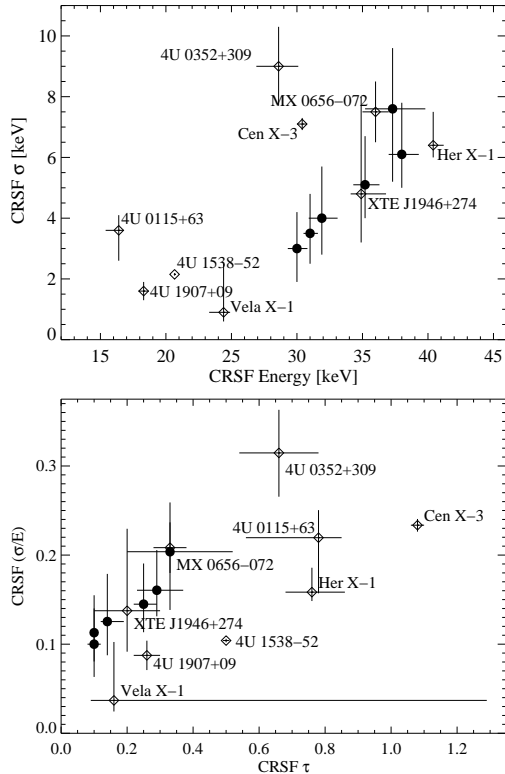


FIGURE 13. Same as Figs. 5 and 6, but with the GX 301–2 phase resolved fits plotted (solid circles).

[40].

CONSIDERATIONS FOR THE NEXT X-RAY TIMING MISSION

Unlike most of the anticipated targets of a next generation timing mission, we do not expect the accreting pulsars to benefit greatly from the ability to measure power spectra to very high (\gtrsim kHz) frequencies. With the exception of photon bubble oscillations [41], these systems are not predicted to have power spectral features in the kHz range. This stems from their large magnetospheric ($\sim 10^{10}$ cm) radii where the accretion disk is truncated and the Keplerian period is of order the neutron star spin period. Minimum timescales are therefore limited to roughly the neutron star spin period, $\sim 0.1\text{--}10^4$ s.

Instead, because their spectra can be time variable and are often strong functions of rotation- (or equivalently, pulse-) phase, the ability to measure the broad band spectrum ($\sim 0.1\text{--}100$ keV) with high significance in a short integration time is the key to future understanding the emission mechanism and cyclotron line formation. For example, if the phase-average spectrum is stable over ~ 10 ks but the spectrum varies in as little as 0.1 in rotation phase, then it is necessary to measure the spectrum in only 1 ks. Large area detectors are therefore not only required for observing high frequency timing features, but are also vital for the study of any source whose spectrum is variable over short timescales. Finally, in order to achieve balanced statistics over the steeply falling pulsar spectra, instrumental effective areas should be heavily weighted toward the high energies. This is particularly important given that all of the known cyclotron lines lie above 10 keV.

REFERENCES

1. Harding, A. K., and Daugherty, J. K., *ApJ*, **374**, 687 (1991).
2. Araya, R. A., and Harding, A. K., *ApJ*, **517**, 334 (1999).
3. Araya-Góchez, R. A., and Harding, A. K., *ApJ*, **544**, 1067 (2000).
4. Isenberg, M., Lamb, D. Q., and Wang, J. C. L., *ApJ*, **505**, 688 (1998).
5. Wheaton, W. A., Doty, J. P., Primini, F. A., Cooke, B. A., Dobson, C. A., Goldman, A., Hecht, M., Howe, S. K., Hoffman, J. A., and Scheepmaker, A., *Nature*, **282**, 240 (1979).
6. Makishima, K., and Mihara, T., “Magnetic Fields of Neutron Stars,” in *Proc. 28th Yamada Conf., Frontiers of X-ray Astronomy*, Universal Acad. Press, Tokyo, 1992, p. 23.
7. Clark, G. W., Woo, J. W., Nagase, F., Makishima, K., and Sakao, T., *ApJ*, **353**, 274 (1990).
8. Kendziorra, E., Mony, B., Kretschmar, P., Maisack, M., Staubert, R., Doebereiner, S., Englhauser, J., Pietsch, W., Reppin, C., and Truemper, J., “Hard X ray observations of VELA X-1 and A0535+26 with HEXE: Discovery of

- cyclotron lines,” in *The Compton Observatory Science Workshop*, 1992, p. 217.
9. Makishima, K., Mihara, T., Ishida, M., Ohashi, T., Sakao, T., Tashiro, M., Tsuru, T., Kii, T., Makino, F., Murakami, T., Nagase, F., Tanaka, Y., Kunieda, H., Tawara, Y., Kitamoto, S., Miyamoto, S., Yoshida, A., and Turner, M. J. L., *ApJ*, **365**, L59–L62 (1990).
 10. Mihara, T., Makishima, K., Kamijo, S., Ohashi, T., Nagase, F., Tanaka, Y., and Koyama, K., *ApJ*, **379**, L61 (1991).
 11. Santangelo, A., del Sordo, S., Segreto, A., dal Fiume, D., Orlandini, M., and Piraino, S., *A&A*, **340**, L55 (1998).
 12. Heindl, W. A., and Chakrabarty, D., “New results on cyclotron lines and neutron star magnetic fields,” in *Highlights in X-ray Astronomy*, 1999, p. 25.
 13. Coburn, W., Heindl, W. A., Gruber, D. E., Rothschild, R. E., Staubert, R., Wilms, J., and Kreykenbohm, I., *ApJ*, **552**, 738 (2001).
 14. Heindl, W. A., Coburn, W., Gruber, D. E., Rothschild, R. E., Kreykenbohm, I., Wilms, J., and Staubert, R., *ApJ*, **563**, L35 (2001).
 15. Heindl, W., Coburn, W., Kreykenbohm, I., and Wilms, J., *ATEL*, **200**, 1 (2003).
 16. Orlandini, M., dal Fiume, D., Frontera, F., del Sordo, S., Piraino, S., Santangelo, A., Segreto, A., Oosterbroek, T., and Parmar, A. N., “BeppoSAX Observations of the X-Ray Binary Pulsar 4u 1626-67,” in *The Active X-ray Sky: Results from BeppoSAX and RXTE*, 1998, p. 158.
 17. Truemper, J., Pietsch, W., Reppin, C., Voges, W., Staubert, R., and Kendziorra, E., *ApJ*, **219**, L105 (1978).
 18. Kendziorra, E., Kretschmar, P., Pan, H. C., Kunz, M., Maisack, M., Staubert, R., Pietsch, W., Truemper, J., Efremov, V., and Sunyaev, R., *A&A*, **291**, L31 (1994).
 19. Clark, G. W., Schmidt, G. D., and Angel, J. R. P., “MX0656-07,” in *IAUC*, 1975, p. 1.
 20. Kaluziński, L. J., “MX 0656-07,” in *IAUC*, 1976, p. 1.
 21. Remillard, R., and Marshall, F., *ATEL*, **197**, 1 (2003).
 22. Morgan, E., Remillard, R., and Swank, J., *ATEL*, **199**, 1 (2003).
 23. Pakull, M. W., Motch, C., and Negueruela, I., *ATEL*, **202**, 1 (2003).
 24. Coburn, W., Heindl, W. A., Rothschild, R. E., Gruber, D. E., Kreykenbohm, I., Wilms, J., Kretschmar, P., and Staubert, R., *ApJ*, **580**, 394–412 (2002).
 25. Coburn, W., *Ph.D. Thesis* (2001).
 26. Makishima, K., Mihara, T., Nagase, F., and Tanaka, Y., *ApJ*, **525**, 978 (1999).
 27. dal Fiume, D., Orlandini, M., del Sordo, S., Frontera, F., Oosterbroek, T., Palazzi, E., Parmar, A. N., Piraino, S., Santangelo, A., and Segreto, A., “The Broad Band Spectral Properties of Binary X-Ray Pulsars,” in *Broad Band X-ray Spectra of Cosmic Sources*, COSPAR/Pergamon Press, New York, 2000, p. 399.
 28. Heindl, W. A., Coburn, W., Gruber, D. E., Pelling, M., Rothschild, R. E., Kretschmar, P., Kreykenbohm, I., Wilms, J., Pottschmidt, K., and Staubert, R., “RXTE Studies of Cyclotron Lines in Accreting Pulsars,” in *Proc. 5th Compton Symp.*, AIP, New York, 2000, p. 178.
 29. Araya, R. A., and Harding, A. K., *ApJ*, **463**, L33+ (1996).
 30. Mészáros, P., and Nagel, W., *ApJ*, **298**, 147 (1985).
 31. White, N. E., Swank, J. H., and Holt, S. S., *ApJ*, **270**, 711 (1983).
 32. Heindl, W. A., Coburn, W., Gruber, D. E., Pelling, M. R., Rothschild, R. E., Wilms, J., Pottschmidt, K., and Staubert, R., *ApJ*, **521**, L49 (1999).
 33. Santangelo, A., Segreto, A., Giarrusso, S., dal Fiume, D., Orlandini, M., Parmar, A. N., Oosterbroek, T., Bulik, T., Mihara, T., Campana, S., Israel, G. L., and Stella, L., *ApJ*, **523**, L85 (1999).
 34. Mihara, T., *Ph.D. Thesis* (1995).
 35. Kreykenbohm, I., Kretschmar, P., Wilms, J., Staubert, R., Kendziorra, E., Gruber, D. E., Heindl, W. A., and Rothschild, R. E., *A&A*, **341**, 141 (1999).
 36. Orlandini, M., dal Fiume, D., Frontera, F., Cusumano, G., del Sordo, S., Giarrusso, S., Piraino, S., Segreto, A., Guainazzi, M., and Piro, L., *A&A*, **332**, 121–126 (1998).
 37. Kreykenbohm, I., Coburn, W., Wilms, J., Kretschmar, P., Staubert, R., Heindl, W. A., and Rothschild, R. E., *A&A*, **395**, 129 (2002).
 38. Leahy, D. A., *MNRAS*, **250**, 310 (1991).
 39. Leahy, D. A., *A&A*, **391**, 219 (2002).
 40. Kreykenbohm, I., Wilms, J., Coburn, W., Kuster, M., Rothschild, R. E., Heindl, W. A., Kretschmar, P., and Staubert, R., “The variable cyclotron line in GX 301-2 (2004), submitted.
 41. Klein, R. I., Arons, J., Jernigan, G., and Hsu, J. J.-L., *ApJ*, **457**, L85 (1996).